

# Direct Investigation of the Dynamics of Charge Recombination Following the Fluorescence Quenching of 9,10-Dicyanoanthracene by Various Electron Donors in Acetonitrile

Eric Vauthey,\* Claudia Högemann, and Xavier Allonas†

*Institute of Physical Chemistry of the University of Fribourg, Pérolles, CH-1700 Fribourg, Switzerland*

*Received: March 4, 1998; In Final Form: May 27, 1998*

The dynamics of the intermediate generated upon diffusional electron transfer (ET) quenching of 9,10-dicyanoanthracene by electron donors of varying oxidation potential in acetonitrile has been investigated using several transient grating techniques. With most of the donor/acceptor pairs studied, the transient grating spectrum cannot be differentiated from those of the free ions. Exciplex fluorescence, with the same lifetime as that of the ion pair, is observed with all donors. To extract from the measured kinetics the rate constant of exciplex dissociation,  $k_{\text{dis}}^{\text{EX}}$ , and of back ET,  $k_{\text{BET}}^{\text{EX}}$ , within these exciplexes, three different schemes have been considered. The best agreement is obtained by assuming that charge recombination predominantly takes place within the exciplex. The obtained  $k_{\text{BET}}^{\text{EX}}$  values are substantially different from the BET rate constants deduced indirectly from the free-ion yields and with a donor-independent rate constant of separation. For each class of donors,  $k_{\text{BET}}^{\text{EX}}$  exhibits a logarithmic free energy dependence with a slope of about  $-2 \text{ eV}^{-1}$ . Moreover,  $k_{\text{dis}}^{\text{EX}}$  is not constant but increases continuously with diminishing donor's oxidation potential.

## Introduction

Over the past decade, there have been a large number of reports of the observation of the inverted region predicted by the Marcus electron transfer (ET) theory.<sup>1–17</sup> In the case of intermolecular ET in solution, this effect appears for the back ET (BET) within geminate ion pairs generated first by diffusional ET quenching.<sup>5–9,11,13,17</sup> In most cases, the rate constant for this process,  $k_{\text{BET}}$ , was not measured directly, but was calculated from the experimentally determined free-ion yield, assuming that  $k_{\text{sep}}$ , the rate constant of ion-pair separation into free ions, was the same for all donor/acceptor pairs.<sup>5,7,11–13,17</sup> In a few studies,  $k_{\text{BET}}$  was measured directly and also exhibited the inversion effect.<sup>8,9</sup> The rate constant for the separation of the ion pair in acetonitrile (MeCN) was determined to range between  $5 \times 10^8 \text{ s}^{-1}$  and  $5 \times 10^9 \text{ s}^{-1}$ , depending on the donor/acceptor pair.<sup>8</sup> More recently, exciplex emissions in MeCN with lifetimes of several nanoseconds have been reported.<sup>18–21</sup> These species can be generated either by direct excitation in the charge transfer (CT) band of the ground-state complex<sup>12</sup> or by diffusional ET quenching of the excited partner.<sup>19–21</sup> The latter route seems to be operative for weakly exergonic ET quenching processes only ( $\Delta G_{\text{ET}} \geq -0.4 \text{ eV}$ ). For more exergonic ET reactions, contact between the reaction partners seems not to be a prerequisite for ET,<sup>22–26</sup> and therefore the ensuing ion pair is often called a loose ion pair (LIP) or a solvent-separated ion pair (SSIP). Exciplexes with full CT character are equivalent to contact ion pairs (CIP), because their absorption spectra are identical to those of the radical ions.<sup>27</sup> It has also been shown that exciplexes with high CT character are characterized by a particularly small rate constant of radiative deactivation.<sup>28</sup>

The determination of the BET rate constants within ion pairs from the free-ion yield was based on the assumption that the nature of intermediate formed upon ET quenching was the same

for all acceptor/donor (A/D) pairs, independently of the exergonicity of the ET quenching, and that  $k_{\text{sep}}$  was also about the same. This procedure is still valid if, albeit exciplexes are formed, charge recombination (CR) only takes place within the LIP formed after dissociation of the exciplex. If this is not the case, the free energy dependence of BET with these systems has to be reexamined.

We report here on direct measurements of the decay rate constants of the intermediate generated upon diffusional ET quenching of 9,10-dicyanoanthracene (DCA) by electron donors of varying oxidation potential in MeCN. These rate constants were determined from transient grating (TG), fluorescence, and photoconductivity measurements. To extract the individual rate constants of BET and separation, several assumptions on the reaction scheme will be considered.

## Experimental Section

**Apparatus.** The ps TG setup has been described in detail previously.<sup>29,30</sup> Briefly, the third harmonic output at 355 nm of an active/passive mode-locked Q-switched Nd:YAG laser (Continuum Model PY61-10) was split into two parts, which, after travelling through different paths of equal lengths, were crossed on the sample. Three different TG techniques were used.

(1) In the spectroscopic mode,<sup>31</sup> the angle of incidence of the pump pulses on the sample was  $0.15^\circ$ . For probing, a 10 mJ pulse at 1064 nm was sent along a variable optical delay line before being focused into a 25 cm long cell filled with a 60:40 (v/v) D<sub>2</sub>O/H<sub>2</sub>O mixture. The resulting white light pulses were collimated on the sample with an angle of incidence of  $0.25^\circ$ . The diffracted signal was focused in a light guide connected to the entrance of a 1/4 m imaging spectrograph (Oriel Multispec). As detector, a  $1024 \times 256$  pixels water-cooled CCD camera (Oriel Instaspec IV) was used.

(2) In the kinetic mode,<sup>32</sup> the angle of incidence of the pump pulses on the sample was the same as above. For probing, a pulse at 532 nm was sent along the variable optical delay line

\* Author to whom correspondence should be addressed. E-mail: Eric.Vauthey@unifr.ch.

† Permanent address: Laboratoire de Photochimie Générale, URA CNRS no. 431, ENSCMu 3, rue A. Werner, 68093 Mulhouse, France.

before being Raman shifted to 681 nm in deuterated DMSO or to 603.5 nm in benzonitrile. The diffracted pulse was filtered through a cutoff filter (Schott RG665 or OG570) and reflected into a vacuum photodiode. At each position of the delay line, the diffracted intensity was averaged over 20 laser pulses. For each measurement, the delay line was scanned eight times. Each measurement was repeated three times and the average value was used.

The transient grating technique is a four-wave mixing method, and therefore the signal intensity depends on the third-order nonlinear optical susceptibility tensor  $\chi^{(3)}$  of the sample.<sup>33</sup> The intensity of the diffracted signal,  $I_{\text{diff}}(t)$ , can be expressed as<sup>34,35</sup>

$$I_{\text{diff}}(t) = C \int_{-\infty}^{+\infty} I_{\text{pr}}(t-t'') \left[ \int_{-\infty}^{t'} \chi_{ijkl}^{(3)}(t''-t') I_{\text{pu}}(t') dt' \right]^2 dt'' \quad (1)$$

where  $C$  is a constant and where  $I_{\text{pr}}$  and  $I_{\text{pu}}$  are the intensities of the probe and pump pulses, respectively.  $\chi_{ijkl}^{(3)}$  is a tensor element of the nonlinear optical susceptibility. Various processes can contribute to  $\chi_{ijkl}^{(3)}$ . These are the electronic and nuclear optical Kerr effects (OKE) from the solvent, the formation of population gratings, and the generation of a density grating due to heat releases. The resulting  $\chi^{(3)}$  tensors have different symmetry properties and can thus be distinguished by using polarization-selective transient grating.<sup>34,35</sup> However, considering the time scale of the experiment, the light intensity, and the geometry used, the only contribution to  $\chi_{ijkl}^{(3)}$  is due to the population gratings. Consequently, when probing at 681 nm,  $\chi_{ijkl}^{(3)}$  is proportional to the concentration of DCA<sup>-</sup>. The second integral in eq 1 represents the convolution of the nonlinear response with the pump pulses, while the first integral is the convolution with the probe pulse. The time profiles of the diffracted intensity were analyzed by iterative reconvolution using eq 1. The temporal width of the pump and probe pulses was determined from the time profile of the diffracted intensity measured in neat CS<sub>2</sub> with focused beams.

(3) In the transient phase grating mode,<sup>30</sup> the angle of incidence of the pump pulses on the sample was 25°. The resulting gratings were probed at 532 nm with an angle of incidence of about 37°. Detection and signal averaging were the same as for the kinetic mode. The time profiles of the diffracted intensity were fitted to the theoretical expression (eq 3 of ref 30 with  $\Delta k = 0$  and  $\Delta n = \Delta n_t$ ). The magnitudes of the acoustic attenuation and of the acoustic frequency were determined from the time profile measured with a solution of 2-hydroxybenzophenone (HBP) in MeCN. In this case, the single heat releasing process is the very fast relaxation of HBP\* to the ground state by reversible intramolecular proton transfer.

The duration of the pulses was about 25 ps. The total pump intensity on the sample was around 2 mJ/cm<sup>2</sup> and the probe pulse intensity was at least 10 times smaller. The polarization of the probe pulse was oriented at 54.7° relative to the polarization of the pump pulses.

Fluorescence lifetime measurements were performed with two different systems.

(1) In the first system, the sample was excited by the third harmonic output of the laser used for TG experiments. The detection was achieved with a pin silicon fast photodiode (Motorola MRD500) connected to a 500 MHz, 2 GS/s digital oscilloscope (Tektronik TDS-620A). The response function of the system had a fwhm of 850 ps. Exciplex emission was selected by using a 570 nm cutoff filter (Schott OG570).

(2) In the second system, based in the Groupe d'Optique Appliquée du CNRS in Strasbourg, the samples were excited

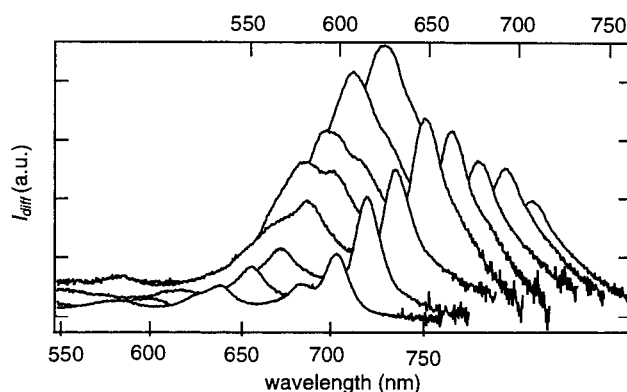


**Figure 1.** TG spectra measured at different time delays after excitation at 355 nm of a solution of DCA and 0.2 M DUR in MeCN (from back to front:  $\Delta t = 60, 300, 470, 600, 750, 1600, 2300,$  and  $3300$  ps. The bottom and top wavelength axes refer to the back and front spectra, respectively).

by the third harmonic of a cw actively mode-locked and cavity dumped Nd:YAG laser. The pulse duration was 84 ps and the average power at 1 kHz was 22 mW. The fluorescence was detected with a streak camera equipped with a 512 channels diode array. The fwhm of the response function was 190 ps.

The exciplex fluorescence was analyzed by assuming a two exponential kinetics with a rising and a decaying component corresponding to exciplex formation and deactivation, respectively.

The free-ion yields were determined using photoconductivity.<sup>36</sup> The photocurrent cell has been described in detail elsewhere.<sup>37</sup> The system benzophenone with 0.02 M 1,2-diazabicyclo[2.2.2]octane in MeCN, which has a free-ion yield of unity,<sup>38</sup> was used as a standard.

**Samples.** 1,2-Diazabicyclo[2.2.2]octane (DABCO) and 9,10-dicyanoanthracene (DCA, Kodak) were purified by sublimation. Biphenyl (BIP), fluorene (FLU), durene (DUR), and pentamethylbenzene (PMB) were recrystallized from ethanol. Mesitylene (MES), *p*-xylene (PXY), anisole (ANI), and veratrole (VER) were distilled. Benzophenone (BP, Aldrich Gold Label) and acetonitrile (UV grade) were used as such. Unless specified, all products were from Fluka. For TG experiments, the absorbance of the sample solution at 355 nm was around 0.15 over 1 mm, the cell thickness. For photoconductivity and fluorescence measurements, the sample absorbance over 1 cm at 355 nm was around 1 and 0.1, respectively. All measurements were performed at  $20 \pm 1$  °C.

## Results

**Population Grating Measurements.** Figure 1 shows the TG spectra obtained at different time delays after excitation at 355 nm of a solution of 9,10-dicyanoanthracene with 0.2 M durene in MeCN. The nature of a TG spectrum has been discussed in ref 31. The diffracted intensity being proportional to the square of the photoinduced changes of absorbance and refractive index, the TG spectrum is the sum of the squares of the absorption and dispersion spectra. The contribution of dispersion to the spectrum leads to a broadening of the bands. This effect is counterbalanced by the band narrowing due to the quadratic dependence of the diffracted intensity on concentration. Consequently the TG spectrum is very similar to the corresponding absorption spectrum. In Figure 1, the TG spectrum at short time delay is dominated by an intense band located around 620 nm and due to <sup>1</sup>DCA\*. As the time delay increases, this band decays and is replaced by a spectrum with bands at 705, 685,

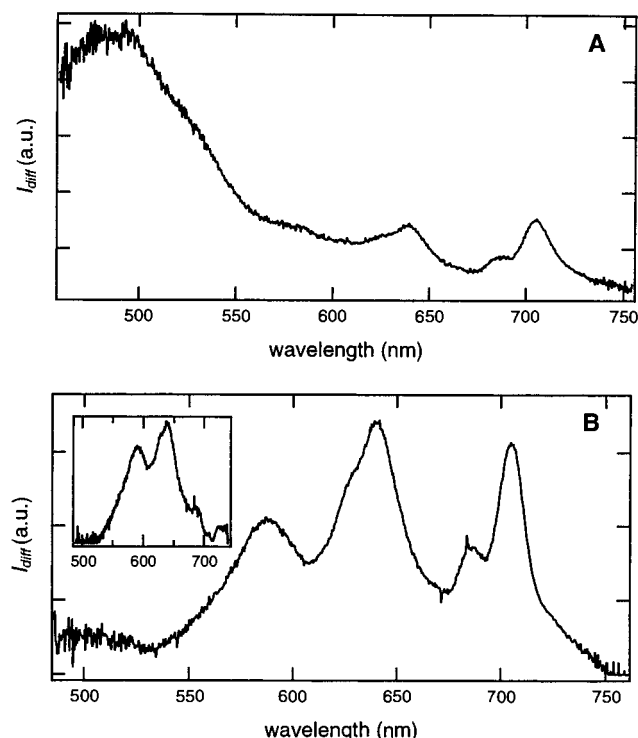


**Figure 2.** TG spectra measured after excitation at 355 nm of a solution of (A) DCA and 0.2 M PMB ( $\Delta t = 1.5$  ns) and (B) DCA and 0.2 M FLU ( $\Delta t = 2.2$  ns) (inset: difference spectrum obtained by subtracting the TG spectrum measured with DCA/DUR from that measured with DCA/FLU).

640, and 580 nm which can all be assigned to  $\text{DCA}^{\bullet-}$ .<sup>39</sup> Depending on the donor (BIP, FLU, PMB), TG bands due to the radical cation could also be observed as shown in Figure 2. DUR cation, which absorbs only weakly around 460 nm, cannot be seen in Figure 1.<sup>40</sup> In the case of BIP and FLU, the TG band of the radical cation overlaps with those of  $\text{DCA}^{\bullet-}$ . Subtracting the TG spectrum with DUR from that measured with BIP and FLU results in a spectrum which can be ascribed to the radical cation (see inset of Figure 2B).<sup>41</sup> The TG spectra measured with ANI and VER are similar to those obtained with DUR. In the case of MES and PXY, the quenching was not complete even after 5 ns, the upper limit of the time window of the experiment. Therefore, the TG spectra at 5 ns exhibit both  $^1\text{DCA}^*$  and  $\text{DCA}^{\bullet-}$  bands. With NAP, MNAP, and DNAP, the intensity of the 580 nm band is much larger than with DUR. This is due to the formation of the dimer radical cation, which absorbs at 580 nm.<sup>42,43</sup> These TG spectra indicate that the species formed by ET quenching of  $^1\text{DCA}^*$  has a strong ionic character. At the present stage, this species will be called an ion pair. Its precise nature will be discussed further on.

The dynamics of this intermediate was investigated by measuring the time evolution of the diffracted intensity at 681 nm. At this wavelength, the diffracted intensity reflects essentially the dynamics of the  $\text{DCA}^{\bullet-}$  population, with additionally, in some cases, that of the cation within the ion pair or as a free ion. At time delays, however,  $^1\text{DCA}^*$  also contributes to the signal. Figure 3 shows the time evolution of the diffracted intensity at 681 nm measured with PMB as electron donor. This time profile has been fitted with eq 1 assuming a three exponential decay of  $\chi_{ijkl}^{(3)}$ : a very fast one, corresponding to the ET quenching of  $^1\text{DCA}^*$  by the donor, a slower one, with a constant  $k_{\text{pop}}$ , due to the decay of the ion-pair population and a very slow one reproducing the constant positive intensity observed at longer time delay and correspond-

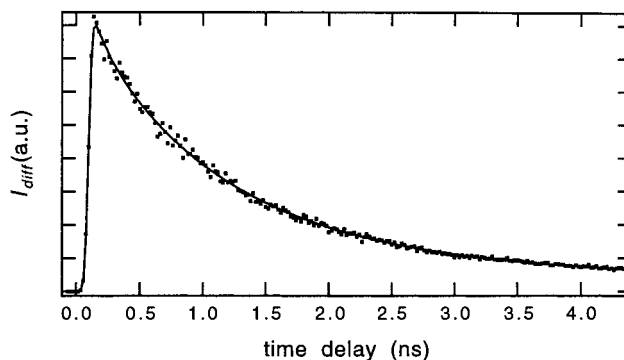


**Figure 3.** Time profile of the diffracted intensity at 681 nm measured with a solution of DCA and 0.3 M PMB in MeCN, and best fit of eq 1.

**TABLE 1: Decay Rate Constants of the Ion-Pair Population,  $k_{\text{pop}}$ , and of the Exciplex Fluorescence,  $k_f^a$**

| donor | $E_{\text{ox}}$<br>(V vs SCE) | $k_{\text{pop}}$<br>( $10^8 \text{ s}^{-1}$ ) | $k_f^a$<br>( $10^8 \text{ s}^{-1}$ ) | $k_{\text{cur}}$ or $k_{\text{slow}}$<br>( $10^8 \text{ s}^{-1}$ ) |
|-------|-------------------------------|---|--------------------------------------|--|
| MES   | 2.11                          |   | 1.15                                 | 1.2  |
| PXY   | 2.06                          |   | 1.2                                  | 1.3  |
| BIP   | 1.96                          |   | 1.6                                  | 1.5  |
| NAP   | 1.80                          |   | 2.1 <sup>50</sup>                    |  |
| DUR   | 1.78                          | 4.8   | 4.9                                  | 4.9  |
| ANI   | 1.76 <sup>79</sup>            | 35  |                                      | >20  |
| PMB   | 1.71                          | 5.3   | 5.3                                  |  |
| FLU   | 1.71                          | 3.1   | 3.3                                  | 3.0  |
| MNAP  | 1.68                          | 3.4 <sup>45</sup>                             | 2.9                                  |  |
| DNAP  | 1.59                          |   | 3.7 <sup>50</sup>                    |  |
| VER   | 1.45 <sup>79</sup>            | 120   |                                      | >20  |

<sup>a</sup> Last column: rate constant of photocurrent build up,  $k_{\text{cur}}$ , (with MES, PXY, and BIP) and rate constant of the heat release due BET,  $k_{\text{slow}}$ , (with the other donors). Unless specified, the oxidation potentials of the donors have been taken from ref 78.

ing to the decay of the free-ion population. In the fit,  $k_{\text{pop}}$  was the only adjustable rate constant. The rate constant for the quenching process was determined at 603.5 nm and the free-ion decay was described by an exponential function with a fixed rate constant of  $10^7 \text{ s}^{-1}$ . This is, of course, not strictly correct as homogeneous ion recombination is a second-order process. However, this assumption is reasonable since free-ion recombination is not operative in the time window of the experiment.

Similar temporal behaviors were observed when DUR, FLU, ANI, and VER were used as donors. The  $k_{\text{pop}}$  values determined with these donors are listed in Table 1. These rate constants are independent of the concentration of donor used except with NAP and its derivatives, MNAP and DNAP, where the observed decay rate constant increases substantially with increasing donor concentration. This effect is due to the reaction of a second donor molecule with the ion pair to generate a transient composed of  $\text{DCA}^{\bullet-}$  and of the corresponding dimer cation.<sup>44,45</sup> The detailed study of this reaction with MNAP has been presented in a previous paper.<sup>45</sup> The value listed in Table 1 for MNAP has been obtained by extrapolating the concentration dependence of  $k_{\text{pop}}$  to zero donor concentration.

The rate constants for the fluorescence quenching of  $\text{DCA}^*$  by weaker donors such as MES, PXY, and BIP are substantially well below the diffusion limit.<sup>46</sup> Even at high donor concentrations, the build up of the ion pair is slow and its decay cannot be measured accurately within the time window of the TG setup, which goes up to 5 ns after excitation.

**Transient Thermal Phase Grating Measurements.** An alternate method to determine the dynamics of the ion pair is to monitor the heat generated upon BET to the neutral ground



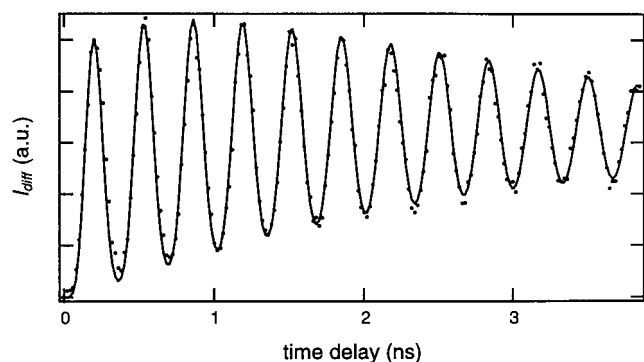


**Figure 4.** Time evolution of the thermal phase grating signal at 532 nm measured with a solution of DCA and 0.3 M DUR in MeCN excited at 355 nm with an angle of incidence of 25°.

state. This can be achieved using the transient thermal phase grating technique.<sup>30,47</sup> In a TG experiment, heat releasing processes, such as internal conversion and exothermic reactions, result in the formation of a density grating and to a corresponding phase grating. The dynamics of the heat releasing process is reflected by the time evolution of the light intensity diffracted from this thermal phase grating, as long as this process is slower than the acoustic response of the sample. The latter depends on the angle of incidence of the pump pulses, on their wavelength, and on the speed of sound in the sample. For this study, the angle of incidence was set to 25°, resulting in an acoustic period of 330 ps. To avoid interferences,<sup>48</sup> the thermal phase grating has to be probed at a wavelength where there is no diffraction by population gratings. Figure 4 shows the time profile of the diffracted intensity measured at 532 nm with a solution of DCA and 0.3 M durene in MeCN. This signal was analyzed assuming three heat releasing processes: (1) a very fast one, within the duration of the pump pulse, corresponding to the release of about 0.61 eV of excess excitation energy; (2) a fast one due to the diffusional ET quenching of DCA\* with a rate constant of  $4.2 \times 10^9 \text{ s}^{-1}$ , determined from the time dependence of the diffracted intensity due to DCA\*; and (3) a slower heat release generated upon BET within the ion pair to the neutral ground state. Four adjustable parameters were used in the fitting procedure: the amount of heat released in the three processes,  $Q_1$  to  $Q_3$ , and the rate constant of the slow heat release,  $k_{\text{slow}}$ . This value is listed in Table 1 for several DCA/D pairs. With ANI and VER, BET was too fast to be distinguished from the other heat releasing processes. If the free-ion yield is known, the enthalpy of ion-pair formation can in principle be determined from the relative magnitudes of the  $Q_n$  values, provided that the amount of heat released in one process is known.<sup>49</sup> In the present case, the relative magnitudes of the  $Q_n$  values showed a substantial variation with the excitation intensity, indicating the occurrence of two-photon absorption. For this reason, no information could be deduced from these values. On the other hand, the  $k_{\text{slow}}$  values were independent of excitation intensity. It can be seen from Table 1 that  $k_{\text{slow}}$  and  $k_{\text{pop}}$ , the decay rate of the ion pair measured in the kinetic mode, are the same within the experimental error.

**Fluorescence Measurements.** Figure 5 shows the decay of the exciplex fluorescence measured with DCA/DUR in MeCN. Exciplex fluorescence was observed with all donors. In the case of ANI and VER, the exciplex emission was substantially weaker than with the other donors.

The decay rate constants of the exciplex emission,  $k_{\text{fl}}$ , are listed in Table 1. The fluorescence quantum yield of all these exciplexes was inferior to 0.05. With BIP, DUR, PMB, and

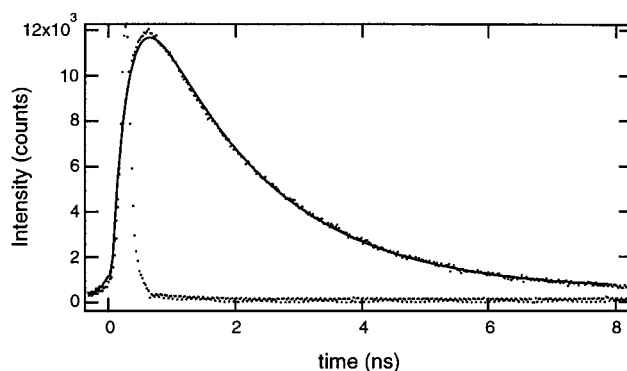


**Figure 5.** Exciplex fluorescence decay measured with a solution of DCA and 0.3 M DUR in MeCN and response function.

**TABLE 2: Free-ion yields normalized to 100% fluorescence quenching,  $\Phi_{\text{ion}}$ , rate constants of separation,  $k_{\text{dis}}^{\text{EX}}$ , and of BET,  $k_{\text{BET}}^{\text{EX}}$ , within the exciplexes in MeCN assuming model (i)**

| donor | $\Phi_{\text{ion}}$ | $k_{\text{dis}}^{\text{EX}} (10^8 \text{ s}^{-1})$ | $k_{\text{BET}}^{\text{EX}} (10^8 \text{ s}^{-1})$ |
|-------|---------------------|--|--|
| MES   | 0.25                | 0.3  | 0.85   |
| PXY   | 0.40                | 0.5  | 0.7  |
| BIP   | 0.5                 | 0.8  | 0.8  |
| NAP   | 0.58 <sup>50</sup>  | 1.2  | 0.9  |
| DUR   | 0.22                | 1.05   | 3.75   |
| ANI   | 0.13                | 4.55   | 30.45  |
| PMB   | 0.18                | 0.95   | 4.35   |
| FLU   | 0.23                | 0.75   | 2.45   |
| MNAP  | 0.47 <sup>45</sup>  | 1.5  | 1.65   |
| DNAP  | 0.33 <sup>50</sup>  | 1.2  | 2.5  |
| VER   | 0.04                | 4.8  | 115.2  |

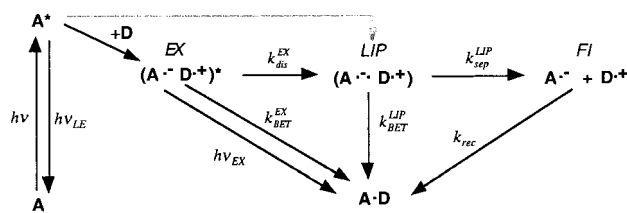
FLU,  $k_{\text{fl}}$  was independent of donor concentration. With NAP, MNAP, and DNAP, a marked increase of  $k_{\text{fl}}$  with concentration was observed. As explained above, this is due to self-quenching. The decay rate constants listed in Table 1 for these donors have been measured at very low donor concentration and taken from ref 50. With MES and PXY, a weak increase of  $k_{\text{fl}}$  with increasing donor concentration has been observed and the values in Table 1 correspond to extrapolation to infinite concentration. This effect indicates the occurrence of the back reaction from the exciplex to the locally excited state. From computer simulation, it appears that the rate constant for this process is in both cases smaller or equal to  $2 \times 10^7 \text{ s}^{-1}$ . In the remaining part of the paper, this process will be neglected since it has no significant influence on the determination of the rate constants for the other deactivation pathways of the exciplex.

With ANI and VER, the emission was too weak to allow accurate lifetime measurements.

**Photoconductivity Measurements.** Most of the free ion yields listed in Table 2 are slightly larger than those reported in ref 7. This is due to the free-ion yield of 0.85 used there for the standard BP/DABCO in MeCN. Recent transient phase grating measurements have shown that the free-ion yield for this system, at a DABCO concentration inferior to 0.3 M, is essentially unity.<sup>38</sup> At higher concentrations, quenching of <sup>1</sup>BP\* by DABCO becomes as fast as intersystem crossing.<sup>51</sup> BET within the ion pair in the singlet state is not spin forbidden and can compete efficiently with separation into free ions. This results in a substantial decrease of the free-ion yield.

With most donors, the rise time of the photocurrent signal was limited by the response time of the photoconductivity setup, of the order of 4 ns. On the other hand, a slower buildup of the signal was observed with MES, PXY, and BIP. The rate constants of photocurrent buildup,  $k_{\text{cur}}$ , for these donors are listed in Table 1. These values, which reflect the buildup of

## SCHEME 1



free-ion population, are equal, within the error limit of  $\pm 5\%$ , to the corresponding  $k_{\text{fi}}$ .

## Discussion

From Table 1, it is immediately clear that the decay rate constant of exciplex emission,  $k_{\text{fi}}$ , and of ion pair population,  $k_{\text{pop}}$ , are identical. These rate constants are also the same as the rate constant of the slow heat release,  $k_{\text{slow}}$  and of photocurrent build up,  $k_{\text{cur}}$ . The concentration dependence of  $k_{\text{fi}}$  measured with MES and PXY is within the error limit of  $k_{\text{cur}}$ . The exciplex formation efficiency in MeCN has been determined to be unity with DUR and PMB, and to decrease steadily with decreasing oxidation potential for stronger donors.<sup>21</sup> Considering the oxidation potential of the donors used here as well as the similitude of  $k_{\text{pop}}$  and  $k_{\text{fi}}$ , the formation efficiency of the corresponding exciplexes must also be unity, with the possible exceptions of DCA/ANI and DCA/VER (vide infra). Consequently, the TG spectra measured after complete quenching of DCA\* are those of the exciplexes. As these spectra cannot be distinguished from those of the radical ions, the CT character of these exciplexes must be large. Such exciplexes are often referred to as CIPs. In the case of DCA/MES and DCA/PXY, the extent of CT might be smaller. For this reason, the transients observed in this study will be called exciplexes. Only those ionic species formed by direct excitation of the ground-state complex will be called CIPs. For the DCA/D pairs investigated here, no absorption band due to such a ground-state complex could be detected.

The possible deactivation pathways of an exciplex are shown in Scheme 1. Apart from fluorescence, the exciplex can either decay to the ground state by a nonradiative transition which is actually a BET, in view of its large CT character, with a rate constant  $k_{\text{BET}}^{\text{EX}}$ , or dissociate to form a LIP with a rate constant  $k_{\text{dis}}^{\text{EX}}$ .

Thus, the exciplex decay constant is given by

$$k_{\text{cur}} = k_{\text{pop}} = k_{\text{slow}} = k_{\text{fi}} = k_{\text{BET}}^{\text{EX}} + k_{\text{dis}}^{\text{EX}} + k_{\text{rad}} \cong k_{\text{BET}}^{\text{EX}} + k_{\text{dis}}^{\text{EX}} \quad (2)$$

where  $k_{\text{rad}}$  is the radiative rate constant of the exciplex. As the fluorescence quantum yields of the exciplexes studied here are inferior to 0.05,  $k_{\text{rad}}$  can be neglected.

The structure of LIP is not really known. This species could be thought of as two diffusing ions at distances where BET is still efficient. In principle, a rate constant of BET within the LIP,  $k_{\text{BET}}^{\text{LIP}}$ , cannot be defined, as BET depends on the interionic distance and as this distance might not be fixed in a LIP.<sup>52–59</sup> The role of the LIP in the CR is rather controversial. Investigations by Mataga and co-workers on CIPs formed by direct excitation of the ground-state complexes revealed that, in most cases, CR was taking place within the CIP only, and that the LIP was not involved in the reaction.<sup>27,60,61</sup> In a few cases, however, CR within the LIP was observed, but  $k_{\text{BET}}^{\text{LIP}}$  was much slower than  $k_{\text{BET}}^{\text{CIP}}$ .<sup>62–64</sup> On the other hand, on the basis of the observation that the variation of DCA/D exciplex lifetime with

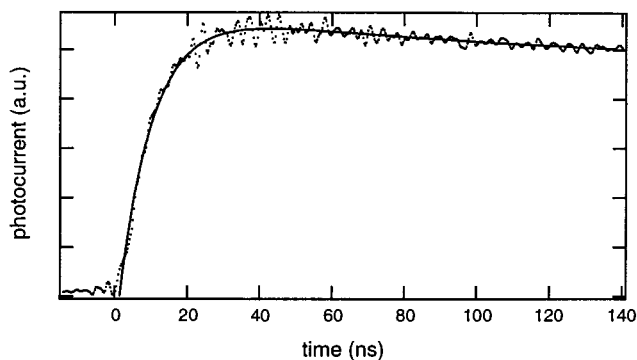


**Figure 6.** Time evolution of the photocurrent measured with a solution of DCA and 0.3 M PXY in MeCN.

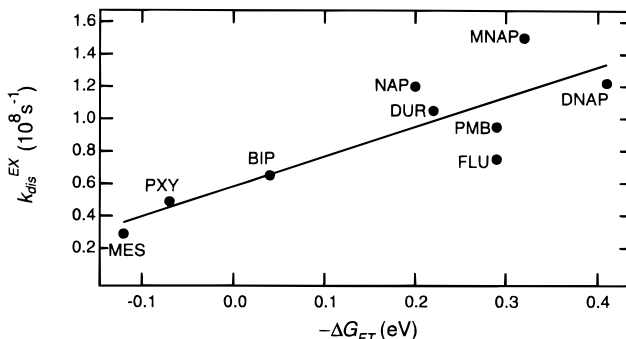


**Figure 7.** Correlation between the rate constant of exciplex dissociation,  $k_{\text{dis}}^{\text{EX}}$ , and the free energy for ET quenching,  $\Delta G_{\text{ET}}$ , assuming model (i). (The  $k_{\text{dis}}^{\text{EX}}$  values for ANI and VER are not included).

the donor oxidation potential was weaker than predicted by Marcus theory for the inverted region, Gould, Farid, and co-workers concluded that dissociation to the LIP was the main deactivation pathway of these exciplexes.<sup>12,18,50</sup> According to these authors, CR essentially takes place within the LIP. This assumption was also based on the analysis of the exciplex fluorescence spectrum of DCA/NAP in MeCN which gave a value for  $k_{\text{BET}}^{\text{EX}}$  of less than  $10^7 \text{ s}^{-1}$ .<sup>44</sup> We will now analyze the data by considering three models: (i) CR takes place within the exciplex only; (ii) CR does only take place within the LIP, and (iii) CR takes place within both the exciplex and the LIP.

**(i) CR Within the Exciplex Only.** Assuming that CR does not take place in the LIP, the free-ion yield,  $\Phi_{\text{ion}}$ , is

$$\Phi_{\text{ion}} = \Phi_{\text{q}} \Phi_{\text{dis}}^{\text{EX}} = \Phi_{\text{q}} \frac{k_{\text{dis}}^{\text{EX}}}{k_{\text{pop}}^{\text{EX}}} \cong \Phi_{\text{q}} \frac{k_{\text{dis}}^{\text{EX}}}{k_{\text{BET}}^{\text{EX}} + k_{\text{dis}}^{\text{EX}}} \quad (3)$$

where  $\Phi_{\text{q}}$  is the quenching efficiency and  $\Phi_{\text{dis}}^{\text{EX}}$  is the dissociation efficiency of the exciplex. The  $k_{\text{dis}}^{\text{EX}}$  and  $k_{\text{BET}}^{\text{EX}}$  values calculated from eq 3 and from the experimentally determined  $\Phi_{\text{ion}}$  are listed in Table 2. For A/D pairs for which both  $k_{\text{pop}}$  and  $k_{\text{fi}}$  were determined, the average value was used in eq 3.

A striking feature of this table is the substantial variation of  $k_{\text{dis}}^{\text{EX}}$  with the oxidation potential of the electron donor. Figure 7 shows the relationship between this rate constant and the free energy for forward ET,  $\Delta G_{\text{ET}}$ , calculated from the Rehm–Weller equation.<sup>65</sup> With the exception of the methoxy-substituted donors, with which a very weak exciplex emission was observed, the rate constant of exciplex dissociation increases almost linearly with the exergonicity of the ET quenching. This effect could originate from the nature of exciplex stabilization. The structure of exciplexes is usually discussed in terms of a linear combination of the CT state  $|A^{\cdot-} D^{\cdot+}\rangle$  and the locally

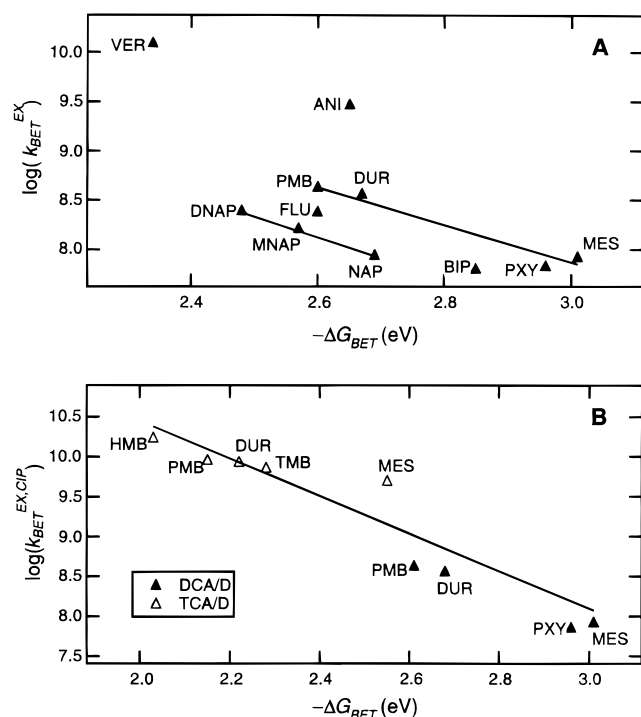


**Figure 8.** Free energy dependence of the rate constant of BET, assuming model (i) (A) within DCA/D exciplexes and (B) within DCA/D exciplexes and TCA/D CIPs (taken from ref 27; HMB: hexamethylbenzene; TMB: 1,2,3,4-tetramethylbenzene).

excited state  $|A^*D\rangle$ .<sup>66,67</sup> The energy of exciplexes with high CT is well correlated with the redox potentials of the constituents. Exciplexes with weaker CT character are more stable than predicted from the redox potentials by an amount  $E_{stab}$  which arises from  $|A^-D^+\rangle \leftrightarrow |A^*D\rangle$  resonance interaction. This interaction becomes significant if either the HOMOs or the LUMOs of A and D have similar energies. The relative energies of these orbitals can be estimated from the  $E_{red}(A) - E_{red}(D)$  and  $E_{ox}(A) - E_{ox}(D)$  differences.<sup>66</sup> The oxidation potential of DCA has been reported to be equal to 1.89 V vs SCE in MeCN.<sup>22</sup> Therefore,  $E_{stab}$  can be expected to be the largest with the weakest electron donors, i.e., with MES, PXY, and BIP. Its magnitude should decrease with the oxidation potential of the donor, i.e., as the free energy of the ET becomes more negative, as observed recently with (dibenzoylmethanato)boron/benzenes complexes.<sup>68</sup> The activation energy for dissociation into free ions must be larger for exciplexes with weak CT character than for exciplexes with an almost complete CT. Recently, Mac et al. determined that the percentage of CT character in the exciplexes composed of DCA/BIP and DCA/DUR was 76% and 87%, respectively.<sup>69</sup> This could lead to the observed free energy dependence of  $k_{dis}^{EX}$ . A similar dependence of the dissociation rate constant on the donor oxidation potential has already been observed with CIPs composed of methyl viologen and naphthalene derivatives in MeCN.<sup>70</sup>

Turning now to the rate constant of BET,  $k_{BET}^{EX}$ , Figure 8A shows that if the A/D pairs are not sorted into different classes, there is no real correlation with the free energy of BET,  $\Delta G_{BET}$ . However, if only donors with similar structures are considered, as the alkylbenzenes and the alkylnaphthalenes, linear relationships between  $\log k_{BET}^{EX}$  and  $\Delta G_{BET}$  are found. A similar free energy dependence of the BET rate constant has also been observed by Mataga and co-workers with CIPs generated by direct excitation in the CT band of the ground-state complex.<sup>27,60–62,71</sup> With the systems studied by these authors, the

slope of the free energy dependence of  $\log k_{BET}^{CIP}$  lies between  $-1$  and  $-1.3$  eV<sup>-1</sup>. Recently, Kochi and co-workers have reported slopes varying from 0 to  $-1.6$  for various types of CIPs.<sup>72</sup> With the systems studied here, slightly larger slopes are obtained,  $-1.9$  eV<sup>-1</sup> for the alkylbenzenes and  $-2.0$  eV<sup>-1</sup> for the alkylnaphthalenes.

According to Tachiya and Murato, this free energy dependence of the BET rate constant is due to the fact that the reaction is controlled by solvent relaxation, the solvation of an exciplex or a CIP directly after excitation of the ground-state complex being far from equilibrium.<sup>73</sup> This explanation cannot be invoked in the present case, first because the BET processes studied here do not take place in the same time scale as dielectric relaxation and second, because the exciplexes are formed by diffusional ET quenching. Moreover, a similar free energy dependence has also been reported for CR in CIPs adsorbed on porous glass.<sup>74</sup>

Gould et al. have also observed such a weak free energy dependence of  $k_{BET}^{CIP}$  with CIPs composed of tetracyanobenzene with various methylbenzene derivatives. The rate constants were discussed in terms of the Marcus theory, and their free energy dependence was ascribed to a simultaneous decrease of the solvent reorganization energy,  $\lambda_s$ , and of the exergonicity of the BET.<sup>75</sup> The decrease of  $\lambda_s$  by going from PXY to hexamethylbenzene (HMB) was explained by the increase of the donor molecular volume with increasing methyl substitution.

On the other hand, Mataga, Miyasaka, and co-workers have observed almost the same free energy dependence of CR within CIPs in polar and nonpolar solvents<sup>71</sup> as well as on porous glass.<sup>74</sup> These authors discussed CR in terms of radiationless transition theory in the weak coupling limit. They concluded that CR within CIPs is dominated mainly by high-frequency intramolecular modes and some low-frequency intracomplex modes and that solvent was of minor importance.

Finally, according to Kochi and co-workers,<sup>72</sup> BET within exciplexes and CIPs is predominantly an inner-sphere process which cannot be analyzed with Marcus theory, which is suited for outer-sphere ET.

In the present case, the extent of CT is not the same in all exciplexes, as suggested by the free energy dependence of  $k_{dis}^{EX}$  and therefore the data can certainly not be discussed in terms of Marcus theory. Moreover, the stabilization of the exciplex by resonance interaction should not be neglected. If this interaction is present, the free energy of exciplex formation,  $\Delta G_{EX}$ , is larger (more negative) than  $\Delta G_{ET}$  by the amount  $E_{stab}$ . Therefore, BET within such an exciplex might be effectively less exergonic than assumed from the magnitude of  $\Delta G_{BET}$ . This effect alone would also make the  $\Delta G_{BET}$  dependence of  $k_{BET}^{EX}$  weaker than predicted by Marcus theory for constant reorganization energy and electron coupling matrix element.

The  $k_{BET}^{EX}$  values are much smaller than the CR rate constants deduced earlier from the magnitude of the free-ion yield using a value for  $k_{sep}$  of  $5 \times 10^8$  s<sup>-1</sup>. In this case, the species generated upon ET quenching was assumed to be a LIP and to have a rate constant of separation independent of the donor oxidation potential. This assumption might be valid for the methoxy-substituted benzenes, ANI and VER. In this case, the exciplex fluorescence is very weak and the rate constant of dissociation is much faster than for the other systems. This rate constant is the same for both ANI and VER which have different oxidation potentials and is very close to the value of  $5 \times 10^8$  s<sup>-1</sup> which is very often used for  $k_{sep}^{LIP}$ . With these donors, quenching could predominantly lead to the formation of the LIP. On the other hand, the fluorescence quantum yield



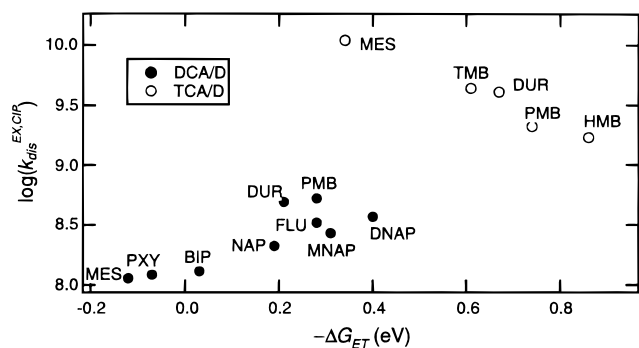


**Figure 9.** Correlation between  $\Delta G_{ET}$  and the rate constant of dissociation of DCA/D exciplexes and TCA/D CIPs (taken from ref 12), assuming model (ii).

of an exciplex with a decay rate constant equal to that measured for the ion-pair population can be expected to be very small (about  $8 \times 10^{-4}$  and  $2 \times 10^{-4}$  with ANI and VER, respectively, assuming the same radiative rate constant as for DCA/DUR). Figure 8A shows that the free energy dependence of BET with these donors is the same as with alkylbenzenes and alkylnaphthalenes. This observation could indicate that the CR mechanism with these two pairs is the same as for the other pairs, although the number of values with methoxybenzenes is certainly too small to draw a definitive conclusion.

Figure 8B shows the free energy dependence of  $k_{BET}^{EX}$  within the exciplexes composed of the methylbenzene derivatives with DCA, measured here, together with the free energy dependence of  $k_{BET}^{CIP}$  within CIPs composed of tetracyanoanthracene (TCA) and various methylbenzene derivatives reported by Asahi et al. The CIPs were formed by direct excitation in the CT band of the ground-state complex. It has been shown that the same intermediates can be generated by diffusional ET quenching of  $^1TCA^*$ .<sup>21</sup> It can be seen that the CR rate constant for DCA/D and TCA/D show almost the same free energy dependence. This supports the assumption made here on the CR with the DCA/D exciplexes.

From the analysis of exciplex emission spectra,  $k_{BET}^{EX}$  within DCA/NAP is smaller than  $10^7 \text{ s}^{-1}$ ,<sup>44</sup> while the  $k_{BET}^{EX}$  value obtained assuming the above scheme is smaller than  $10^8 \text{ s}^{-1}$ . Considering that CR within CIPs can be even faster than  $10^{12} \text{ s}^{-1}$ ,<sup>60,76</sup> the  $k_{BET}^{EX}$  value obtained here is not totally inconsistent with the calculated one.

**(ii) CR within LIP Only.** The exponential decay of the ion-pair population and its close similarity with the exciplex emission decay can also be explained in terms of a scheme where the exciplex decays only by dissociation to the LIP, i.e.,  $k_{dis}^{EX} \gg k_{BET}^{EX}$ , and where both  $k_{sep}^{LIP}$  and  $k_{BET}^{LIP}$  are larger than  $k_{dis}^{EX}$ . In this case, the LIP decays faster than it is formed and the exciplex dissociation acts as a bottleneck. The free-ion yield is thus controlled by the relative magnitudes of  $k_{sep}^{LIP}$  and  $k_{BET}^{LIP}$ , i.e., the formation of an exciplex upon diffusional quenching has no influence on the CR dynamics.  $k_{sep}^{LIP}$  and  $k_{BET}^{LIP}$  cannot be extracted from the free-ion yield unless one of them is known. If  $k_{sep}^{LIP}$  is assumed to be the same for all LIPs, the same  $k_{BET}^{LIP}$  values as those already reported from indirect measurements are obtained.<sup>5,7,11</sup> However, according to the direct measurements of Mataga and co-workers, the magnitude of  $k_{sep}^{LIP}$  varies from one LIP to the other without any evident trend.<sup>8</sup>

If this scheme is valid, the measured population decay rate constants are equal to  $k_{dis}^{EX}$ . As in model (i),  $k_{dis}^{EX}$  is free energy dependent, but the dependence is now substantially larger. Figure 9 shows the free energy dependence of  $k_{dis}^{EX} = k_{pop}$  with the

DCA/D pairs together with the free energy dependence of  $k_{dis}^{CIP}$  with TCA/D pairs reported by Gould et al. from indirect measurements.<sup>12</sup> As mentioned above, the same species can be formed either by direct excitation of the ground-state complex or by diffusional ET quenching of  $^1TCA^*$ . Not only the dissociation rate constants with TCA/D do not fit on the same line, but they show an opposite trend. It is difficult to find an explanation for this very different behavior of DCA/D and TCA/D.

**(iii) CR within Both Exciplex and LIP.** Assuming that CR is taking place within both the exciplex and the LIP, the free-ion yield is given by

$$\Phi_{ion} = \Phi_q \Phi_{dis}^{EX} \Phi_{sep}^{LIP} \quad (4)$$

where  $\Phi_{sep}^{LIP}$  is the separation efficiency of the LIP. Considering the separation rate constant measured with other LIPs,  $k_{sep}^{LIP}$  must be substantially larger than  $k_{dis}^{EX}$ .<sup>8</sup> This is quite reasonable, as the A/D interactions are certainly smaller in a LIP than in an exciplex. Scheme 1 and model (ii) are based on the assumption that the LIP is a true intermediate with a well-defined geometry and a unique lifetime. This description of the LIP is very helpful but might not be fully correct. Indeed, a LIP should be rather thought of as two diffusing ions at distance where BET is still possible. Considering the distance dependence of the solvent reorganization energy,  $\lambda_s$ , in Marcus theory, the optimal interionic distance for the fastest BET depends on the free energy of the reaction. At large exergonicity ( $-\Delta G_{BET} > \lambda$ ), there is a range of distances where the decrease of the activation barrier with increasing distance can overcome the simultaneous falloff of the electron coupling matrix element. After exciplex dissociation, the ions diffuse away and reach the range of distance where BET is the fastest. In the same way, diffusion becomes faster because of the decrease of the activation barrier with interionic distance. Therefore the probability for CR at a distance  $d$  depends on the relative magnitude of the BET rate constant at  $d$  and of the diffusion rate constant at  $d$ . If diffusion increases much faster with distance than does BET, CR will take place within the exciplex only. Otherwise, CR within the LIP can take place as well. In this case, the kinetics of CR within the LIP might be no longer exponential. According to Kakitani and co-workers, this effect should lead to a root inverse tail ( $t^{-1/2}$ ) in the kinetics of the ion-pair population.<sup>77</sup> Considering our experimental time window (0–5 ns), this component might be difficult to observe and could be missed so that  $\Phi_{dis}^{EX}$  might be slightly underestimated. If this is the case, the actual  $k_{dis}^{EX}$  values are slightly larger than those listed in Table 2, while the actual  $k_{BET}^{EX}$  values are smaller than those listed in this table. In principle, the importance of this effect should increase with increasing CR exergonicity and be thus more marked with MES, PXY, and BIP. In this case, the free energy dependence of both  $k_{BET}^{EX}$  and  $k_{dis}^{EX}$  could be slightly smaller than those determined assuming model (i). However, considering the close similarity between the emission lifetimes of exciplexes with MES, PXY, and BIP and the photocurrent buildup times, the role of the LIP in the CR process must be of minor importance for the systems studied here.

## Conclusion

From the above discussion, it appears that the data obtained in this investigation are better explained with a scheme where CR predominantly takes place within the exciplex formed by diffusional quenching [model (i)], although the other models cannot be completely ruled out. The rate constants of BET,

calculated assuming model (i), for A/D pairs forming an exciplex are very different from the values determined from the free-ion yields with a unique and donor-independent rate constant of separation. This procedure might be valid for A/D systems for which ET quenching is more exergonic and results directly in the formation of a LIP. The free energy dependence of BET within pairs forming exciplexes is very similar to that already reported for CIPs generated by direct excitation of the ground-state complex. For this reason, when studying the free energy dependence of CR, exciplex-forming pairs should not be treated as pairs forming directly a LIP. If this distinction is not made, the analysis of free energy dependence of BET rate constants measured with an ensemble of A/D pairs comprising both types of systems might be flawed.

**Acknowledgment.** This work was supported by the *Fonds national suisse de la recherche scientifique* through Project 20-49235.96 and by the *program d'encouragement à la relève universitaire de la Confédération*. Financial support from the *Fonds de la recherche* and the *Conseil de l'Université de Fribourg* is also acknowledged.

## References and Notes

- Miller, J. R.; Beitz, J. V.; Huddleston, R. K. *J. Am. Chem. Soc.* **1984**, *106*, 5057.
- Miller, J. R.; Calcaterra, L. T.; Closs, G. L. *J. Am. Chem. Soc.* **1984**, *106*, 3047.
- Wasielewski, M. R.; Niemczyk, N. P.; Svec, W. A.; Pewitt, E. B. *J. Am. Chem. Soc.* **1985**, *107*, 1080.
- Irvine, M. P.; Harrison, R. J.; Beddard, G. S.; Leighton, P.; Sanders, J. K. M. *Chem. Phys.* **1986**, *104*, 315.
- Gould, I. R.; Ege, D.; Mattes, S. L.; Farid, S. *J. Am. Chem. Soc.* **1987**, *109*, 3794.
- Ohno, T.; Yoshimura, A.; Shioyama, H.; Mataga, N. *J. Phys. Chem.* **1987**, *91*, 4365.
- Vauthey, E.; Suppan, P.; Haselbach, E. *Helv. Chim. Acta* **1988**, *71*, 93.
- Mataga, N.; Asahi, T.; Kanda, Y.; Okada, T.; Kakitani, T. *Chem. Phys.* **1988**, *127*, 249.
- Levin, P. P.; Pluzhnikov, P. F.; Kuzmin, V. A. *Chem. Phys. Lett.* **1988**, *147*, 283.
- Chen, P.; Duesing, R.; Tapolsky, G.; Meyer, T. J. *J. Am. Chem. Soc.* **1989**, *111*, 8305.
- Kikuchi, K.; Takahashi, Y.; Hoshi, M.; Niwa, T.; Katagiri, T.; Miyashi, T. *J. Phys. Chem.* **1991**, *95*, 2378.
- Gould, I. R.; Young, R. H.; Moody, R. E.; Farid, S. *J. Phys. Chem.* **1991**, *95*, 2068.
- Grampp, G.; Hetz, G. *Ber. Bunsen-Ges. Phys. Chem.* **1992**, *96*, 198.
- Kapturkiewicz, A. *Chem. Phys.* **1992**, *166*, 259.
- Larson, S. L.; Cooley, L. F.; Elliott, C. M.; Kelley, D. F. *J. Am. Chem. Soc.* **1992**, *114*, 9504.
- Yonemoto, E. H.; Riley, R. L.; Kim, Y. I.; Atherton, S. J.; Schmehl, R. H.; Mallouk, T. E. *J. Am. Chem. Soc.* **1992**, *114*, 8081.
- Burget, D.; Jacques, P.; Vauthey, E.; Suppan, P.; Haselbach, E. *J. Chem. Soc., Faraday Trans.* **1994**, *90*, 2481.
- Gould, I. R.; Farid, S. *J. Phys. Chem.* **1992**, *96*, 7635.
- Kikuchi, K.; Niwa, T.; Takahashi, Y.; Ikeda, H.; Miyashi, T.; Hoshi, M. *Chem. Phys. Lett.* **1990**, *173*, 421.
- Kuzmin, M. G.; Sadovskii, N. A.; Weinstein, J.; Kutsenok, O. *Proc. Indian Acad. Sci., Chem. Sci.* **1993**, *105*, 637.
- Gould, I. R.; Young, R. H.; Mueller, L. J.; Farid, S. *J. Am. Chem. Soc.* **1994**, *116*, 8176.
- Kikuchi, K.; Niwa, T.; Takahashi, Y.; Ikeda, H.; Miyashi, T. *J. Phys. Chem.* **1993**, *97*, 5070.
- Scully, A. D.; Takeda, T.; Okamoto, M.; Hirayama, S. *Chem. Phys. Lett.* **1994**, *228*, 32.
- Murata, S.; Nishimura, M.; Matsuzaki, S. Y.; Tachiya, M. *Chem. Phys. Lett.* **1994**, *200*, 219.
- Jacques, P.; Allonas, X. *Chem. Phys. Lett.* **1995**, *233*, 533.
- Matsuda, N.; Kakitani, T.; Denda, T.; Mataga, N. *Chem. Phys.* **1995**, *190*, 83.
- Asahi, T.; Mataga, N.; Takahashi, Y.; Miyashi, T. *Chem. Phys. Lett.* **1990**, *171*, 309.
- Gould, I. R.; Young, R. H.; Mueller, L. J.; Albrecht, A. C.; Farid, S. *J. Am. Chem. Soc.* **1994**, *116*, 8188.
- Vauthey, E. *Chem. Phys. Lett.* **1993**, *216*, 530.
- Vauthey, E.; Henseler, A. *J. Phys. Chem.* **1995**, *99*, 8652.
- Högemann, C.; Pauchard, M.; Vauthey, E. *Rev. Sci. Instrum.* **1996**, *67*, 3449.
- Gumy, J.-C.; Vauthey, E. *J. Phys. Chem.* **1996**, *100*, 8628.
- Shen, Y. R. *The Principles of Nonlinear Spectroscopy*; J. Wiley: New York, 1984.
- Etchepare, J.; Grillon, G.; Chambaret, J. P.; Hamoniaux, G.; Orzag, A. *Opt. Commun.* **1987**, *63*, 329.
- Deeg, F. W.; Fayer, M. D. *J. Chem. Phys.* **1989**, *91*, 2269.
- Vauthey, E.; Pilloud, D.; Haselbach, E.; Suppan, P.; Jacques, P. *Chem. Phys. Lett.* **1993**, *215*, 264.
- von Raumer, M.; Suppan, P.; Jacques, P. *J. Photochem. Photobiol. A* **1997**, *105*, 21.
- Henseler, A.; Vauthey, E. *J. Photochem. Photobiol. A* **1995**, *91*, 7.
- Haselbach, E.; Vauthey, E.; Suppan, P. *Tetrahedron* **1988**, *44*, 7335.
- Bockman, T. M.; Karpinski, Z. J.; Sankararaman, S.; Kochi, J. *J. Am. Chem. Soc.* **1992**, *114*, 1970.
- Shida, T. *Electronic Absorption Spectra of Radical Ions*; Elsevier: Amsterdam, 1988; Vol. Physical Sciences data 34.
- Rodgers, M. A. J. *J. Chem. Soc., Faraday Trans. 1* **1972**, 1278.
- Gschwind, R.; Haselbach, E. *Helv. Chim. Acta* **1979**, *62*, 941.
- Gould, I. R.; Farid, S. *J. Am. Chem. Soc.* **1993**, *115*, 4814.
- Vauthey, E. *J. Phys. Chem. A* **1997**, *101*, 1635.
- Pilloud, D. PhD Thesis, University of Fribourg, Fribourg, Switzerland, 1993.
- Genberg, L.; Bao, Q.; Gracewski, S.; Miller, R. J. D. *Chem. Phys.* **1989**, *131*, 81.
- Vauthey, E.; Henseler, A. *J. Photochem. Photobiol. A* **1998**, *112*, 103.
- Vauthey, E.; Henseler, A. *J. Phys. Chem.* **1996**, *100*, 170.
- Gould, I. R.; Farid, S. *J. Am. Chem. Soc.* **1993**, *115*, 4814.
- Peters, K. S.; Lee, J. J. *J. Phys. Chem.* **1993**, *97*, 3761.
- Baba, H.; Goodman, L.; Valenti, P. C. *J. Am. Chem. Soc.* **1966**, *88*, 5410.
- Burshtein, A. I. *J. Chem. Phys.* **1995**, *103*, 7927.
- Burshtein, A. I.; Krissinel, E. *J. Phys. Chem.* **1996**, *100*, 3005.
- Burshtein, A. I.; Shokhirev, N. V. *J. Phys. Chem.* **1997**, *101*, 25.
- Murata, S.; Tachiya, M. *J. Phys. Chem.* **1996**, *100*, 4064.
- Swallen, S. F.; Fayer, M. D. *J. Chem. Phys.* **1995**, *103*, 8864.
- Swallen, S. F.; Weidemaier, K.; Fayer, M. D. *J. Chem. Phys.* **1996**, *104*, 2976.
- Swallen, S. F.; Weidemaier, K.; Tavernier, H. L.; Fayer, M. D. *J. Phys. Chem.* **1996**, *100*, 8106.
- Asahi, T.; Mataga, N. *J. Phys. Chem.* **1989**, *93*, 6575.
- Asahi, T.; Mataga, N. *J. Phys. Chem.* **1991**, *95*, 1956.
- Ojima, S.; Myasaka, H.; Mataga, N. *J. Phys. Chem.* **1990**, *94*, 7534.
- Peters, K. S.; Lee, J. J. *J. Phys. Chem.* **1992**, *96*, 8941.
- Peters, K. S.; Lee, J. J. *J. Am. Chem. Soc.* **1993**, *115*, 3643.
- Rehm, D.; Weller, A. *Isr. J. Chem.* **1970**, *8*, 259.
- The Exciplex*; Weller, A., Ed.; Academic Press: New York, 1975; p 23.
- Organic Molecular Photophysics*; Beens, H. Weller, A., Eds.; John Wiley: New York, 1975; Vol. 2, p 159.
- Chow, Y. L.; Johansson, C. I. *J. Phys. Chem.* **1995**, *99*, 17558.
- Mac, M.; Kwiatkowski, P.; Turek, A. M. *Chem. Phys. Lett.* **1996**, *250*, 104.
- Hubig, S. M. *J. Phys. Chem.* **1992**, *96*, 2903.
- Asahi, T.; Ohkohchi, M.; Mataga, N. *J. Phys. Chem.* **1993**, *97*, 13152.
- Hubig, S. M.; Bockman, T. M.; Kochi, J. K. *J. Am. Chem. Soc.* **1996**, *118*, 3842.
- Tachiya, M.; Murata, S. *J. Am. Chem. Soc.* **1994**, *116*, 2434.
- Miyasaka, H.; Kotani, S.; Itaya, A.; Schweitzer, G.; Schryver, F. C. D.; Mataga, N. *J. Phys. Chem. B* **1997**, *101*, 7978.
- Gould, I. R.; Noukakis, D.; Gomez-Jahn, L.; Goodman, J. L.; Farid, D. *J. Am. Chem. Soc.* **1993**, *115*, 4405.
- Wynne, K.; Galli, C.; Hochstrasser, R. M. *J. Chem. Phys.* **1994**, *100*, 4797.
- Yoshimori, A.; Watanabe, K.; Kakitani, T. *Chem. Phys.* **1995**, *201*, 35.
- Gould, I. R.; Ege, D.; Moser, J. E.; Farid, S. *J. Am. Chem. Soc.* **1990**, *112*, 4290.
- Zweig, A.; Hodson, W. G.; Jura, W. H. *J. Am. Chem. Soc.* **1964**, *86*, 4124.